SC5099 (ID02) report – Strain hardening in colloidal gels

W. J. Smit,[1] T. Divoux,[1] S. Manneville,[1] L. Matthews,[2] T. Narayanan,[2] E. Del Gado,[3] and T. Gibaud[1]

[1] *Univ Lyon, Ens de Lyon, Univ Claude Bernard, CNRS, Laboratoire de Physique, F69342 Lyon, France*

[2] *ESRF, The European Synchrotron, F-38043 Grenoble Cedex, France*

[3] *Department of Physics, Institute for Soft Matter Synthesis and Metrology, Georgetown University, USA*

(Dated: September 10, 2021)

During the run SC5099 on ID02 from april 2nd to april 5th 2021 we measured the gelation properties of three different colloidal dispersion composed of different silica colloidal particles (Ludox SM, HS and TM). Both rheology and TRSAXS show that the linear mechanics and structural properties of the tree dispersion can be mapped on master curves underlying similar properties. However the rupture properities of the gel during gelation greatly differ: gel composed of large particles show typiral yielding behavior whereas gel composed of smaller particles display strain hardening behavior (an increase of the elastic properties before rupture). Those results show that such non-linear mechanical properties cannot be related to classical structural properties such as the gel cluster size and their fractal dimension. Emmanuela Del Gado from Georgetown University (USA) is currently exploring this behavior with simulation. Her preliminary results seems to show that the pertinent parameters are the branching and bending modulus of the gel network. Showing and understanding strong strain hardening in colloidal gel is new and hopefully will lead to a high impact publication in the next few months.

PACS numbers: xxx

I. INTRODUCTION

Colloidal gels are soft solids whose structure is composed of attractive colloids that form a space-spanning network. Colloidal gels display mainly solid-like properties at rest and under mild deformations. However, upon increasing external mechanical constraints, their viscoelastic response becomes non-linear and generally involves a yield point above which they break and flow. Prior to yielding, most gels become weaker in the non-linear regime. Yet, some gels show the reverse trend: their elastic modulus G' increases as the imposed strain or stress increases, i.e., these gels "harden" until abrupt rupture takes place. Such strain hardening has been reported in a wide range of materials including rubbers,polymer gels and semi-flexible biopolymer networks [1–3]. In colloidal gels, however, strain hardening is rather rare and, when present, its amplitude is usually small, with G' increasing at most by a factor of 5. This is the case for gels of polystyrene particles [4] or for sodium caseinate gels [5]. Still, our previous results on natural rubber latex gels [6] as well as other works on thermosensitive polystyrene gels [7] and our recent preliminary experiments on silica gels display a strain-hardening behaviour by a factor of 10 to 100, comparable to biopolymer gels.

In this study we characterized the mechanical and structural properties of three different gels and show that the pertinent parameters to understand stain hardening are not typical structural characteristics like the cluster sizes or the fractal dimension of gel network but rather the branching and the bending modulus of the gel strand [8] (work in progress in collaboration with Emanuela Del Gado)

II. MATERIALS AND METHODS

We prepare three different colloidal gels composed oif ludox particles of mean radius r_0 and final volume fraction ϕ. r_0 is measured using SAXS in the very dilute regime. Sodium chloride at a concentration [NaCl] is added to the dispersion to screen the repulsive potential between the negatively charged silica particles and induces the aggregation. For gel composed of SM ludox particles: $r_{0,SM} = 5.3$ nm, $\phi_{SM} = 2.5\%$ and [NaCl]=500 mM. For gel composed of HS ludox particles: $r_{0,HS} = 8.3$ nm, $\phi_{HS} = 5\%$ and [NaCl]=610 mM. For gel composed of TM ludox particles: $r_{0,TM} = 12.9$ nm, $\phi_{TM} = 10\%$ and [NaCl]=700 mM . The volume fraction and salt content was chosen so that the gelation take place within 1 h : $t_{g,SM} = 1200 \pm 200$ s, $t_{g,HS} = 3000 \pm 400$ s, $t_{g,TM} = 1860 \pm 180$ s. Measurements were performed in a Couette cell at room temperature 20°C and time resolved small angle X-ray scattering (TRUSAXS) was performed at the ESRF on beamline ID02. The mixing of the ingredient define the starting time of the experiment, $t = 0$ s.

III. MECHANICAL PROPERTIES

As shown in Fig. 1, for all the three dispersion, the loss G'' and elastic G' increase with time. At short time scales $G'' > G'$, the sample is fluid whereas at long time scales $G' > G''$, the sample is a soft solid. We define the gelation point at $t = t_g$ when $G' = G''$. All the measurements scale on a master curve when the axis are normalized by the gelation parameters (t_g, G_g) The color code.

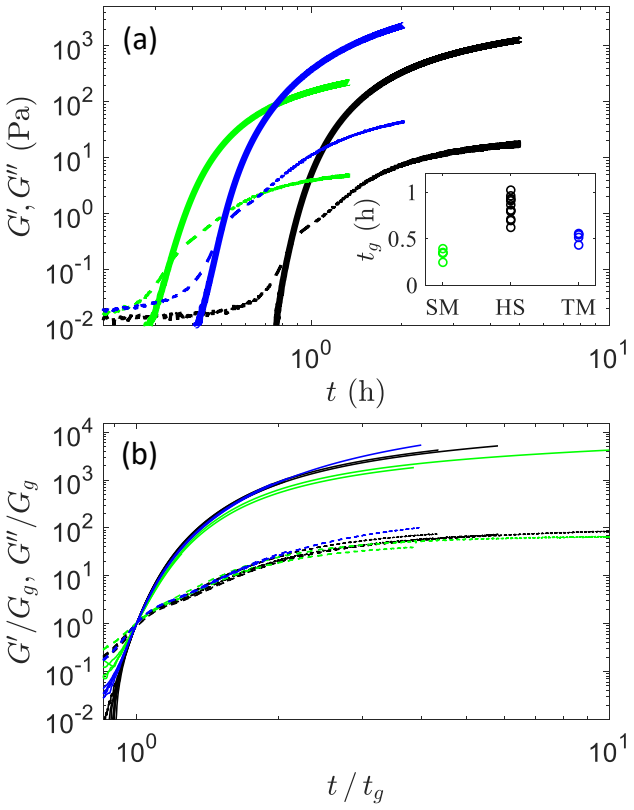

FIG. 1. . Evolution of the viscoelastic modulus of the ludox dispersions during gelation. (a) Typical evolution of the elastic G' (line) and loss modulus G'' (dash line) for SM (green), HS (black) and TM (blue) dispersions. The inset show the measured gelation time t_g which correspond at time when $G' = G'' = G_g$. (b) G'/G_g (line), G''/G_g (dash line) as function of the normalized time t/t_g for the the three ludox dispersions. Measurements were carried out in the linear regime at $f = 1$ Hz for a strain amplitude of $\gamma_0 = 1\%$.

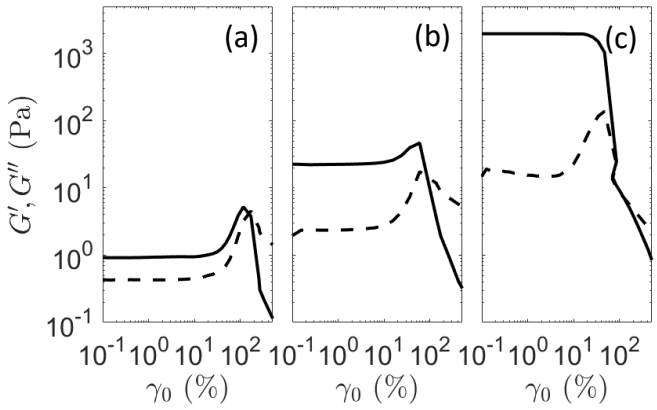

FIG. 2. Non-linear rheology for ludox HS dispersions. strain sweep experiment showing the evolution the viscoelastic modulus G' (line) and G'' (dash line) as a function of the strain amplitude γ_0 measured at $f = 1$ Hz at different times $t > t_g$: (a) $t/t_g = 1.15$. (a) $t/t_g = 1.42$ (a) $t/t_g = 14$.

The non-linear mechanical properties of the dispersions are probed using fast strain sweep experiments performed at different times after the gelation time t_g, Fig. 2. As the strain amplitudes increases G'' overcome the G' and the gels fluidize. Before the yielding point at γ_y when $G' = G''$, we observe strain hardening: G' and G'' increases. This effect is all the more important that the strain sweep experiment is performed close to t_g. This behavior is quantified by the elastic and viscous strain hardening factor $\Delta G'/G'_0$ and $\Delta G''/G''_0$. $\Delta G'$ is defined by the difference between G'_0 the elastic modulus of the gel in the linear regime and the maximum of G' before the yielding point. The same definition holds for the viscous strain hardening factor using G'' instead of G'.

This strain hardening effect is observed in all the three ludox gels and their strain hardening factors are displayed in Fig. 3. We observe that $\Delta G'/G'_0$ is maximum just after t_g and decreases monotonically with time. This effect is all the more important that the size of the particles composing the gel is small.: close to t_g for SM gels, $\Delta G'/G'_0 \sim 20$ whereas to TM gels $\Delta G'/G'_0 \sim 2$. A strain hardening factor of 20 is remarkable. In typical colloidal gel strain hardening is rarely observed and its value is usually of the order of 2 [4]. However the strain hardening effect vanishes for mature gels at large t/t_g except for SM gels where the phenomena persists. The fact that this strain hardening effect is transient explains why it is rarely observed in colloidal gels.

As shown in Fig. 3b the viscous dissipation factor $\Delta G''/G'_0 \sim 10$ remains constant in time and is independent of the ludox dispersion. The strain hardening is only an elastic effect.

To better comprehend those new results we characterized the gelation process using TRUSAXS. In other words, can we understand those results in terms of cluster size or fractal dimensions?

IV. STRUCTURAL PROPERTIES

We measured the scattered intensity $I(q,t)$ as function of the wave number q and the time t, Fig. 4. As time increases, we observe an increase of the forward scattering. This increase is typical of the gelation process: the colloids aggregate and form clusters that grow over time. We fit the data using a mass fractal model [9]:

$$I(q) = P(q)\left[1 + \frac{d_f\ \Gamma(d_f-1)}{[1+1/(q\xi)^2\ ]^{(d_f-1)/2}} \frac{\sin[(d_f-1)\tan^{-1}(q\xi)]}{(qr_0)^{d_f}}\right],$$

$P(q)$ being the form factor of the ludox particles of radius r_0 and the parameters $(\xi,\ d_f)$ being the size and the fractal dimensions of the clusters.

As shown in Fig. 5, we have plotted ξ and d_f as function of the normalized time t/t_g for the three dispersions. Smaller particles form larger clusters: SM ludox of radius of gyration $r_{0,SM} = 5.3$ nm form clusters as large as $\xi = \xi_\infty = 272$ nm for $t >> t_g$, i.e. ~ 50 times larger a single colloid whereas larger ludox particles form smaller

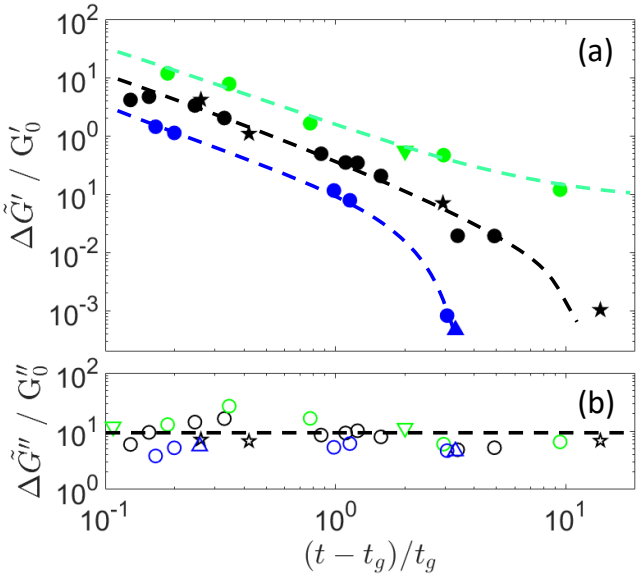

FIG. 3. Strain hardening parameters for the three ludox gels (SM (green), TM (blue) and HS (black). Evolution of the elastic and viscous strain hardening factor repectively in (a) $\Delta G'/G'_0$ and (b) $\Delta G''/G''_0$ as a function of the reduced time $(t-t_g)/t_g$.

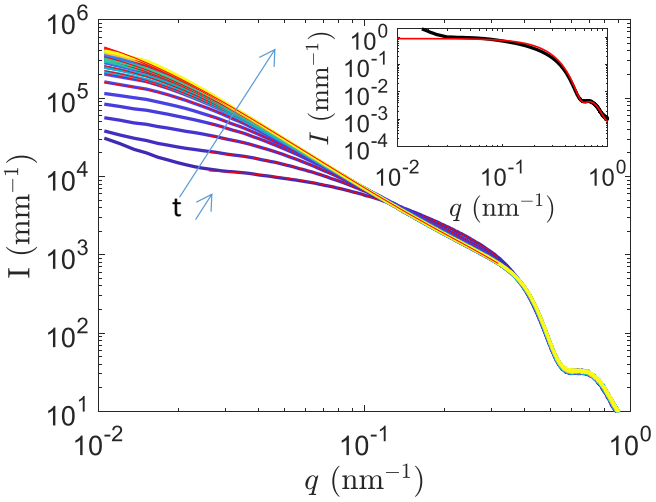

FIG. 4. Time evolution of the scattering intensity $I(q,t)$ as a function of the scattering wave vector q for the HS ludox dispersion. The color codes from blue to yellow for the time. Red lines as mass fractal fits. Measurements where perfomed using rheo-saxs and the gelation time t_g was obtained from the rheology data. Inset: form factor of the HS particle dispersed in deionized water at a volume fraction of 0.1 %. The red line corresponds to a polydisperse hard sphere fit with a radius of gyration of $r_0 = 8.3$ nm and a polydispersity of 13%.

clusters: TM ludox of radius of gyration $r_{0,TM} = 12.9$ nm form clusters of maximum size $\xi = \xi_\infty = 39$ nm, i.e. only ~ 3 times larger than a single colloid. The time evolution of the three ludox dispersions follow a similar trend and can be mapped on a single master curve when we plot $(\xi - r_0)/\xi_\infty$ as a function of the normalized time. In all the three dispersions, the clusters become rapidly fractal and reach a fractal dimension $d_f \sim 2.2$ typical of a reaction limited cluster aggregation (RLCA) process.

We finally turn our attention to experiments where the structure of the dispersion was measured while performing a strain sweep experiments. We used rheo-TRUSAXS and rheo-video to check for characteristic changes in micro-structure and the macro-structure (millimeter) respectively as the strain amplitude γ_0 is increased from the linear to the non-linear regime. rheo-TRUSAXS experiment consist in strain sweep experiment with a simultaneous measured the scattered intensity in the tangential position. A preliminary analysis is displayed in Fig. 6. In the strain hardening regime, $I(q)$ in the $q-$range tested is very similar to $I(q)$ in the linear regime. Structural changes, if there is any, might happen at larger scales. To check this hypothesis we recorded images of the strain sweep experiment in a transparent couette cell with a ~ 1 mm resolution, Fig. 7. Preliminary analysis show that the gel remains homogeneous at those millimetric scales until yielding at γ_y. Above γ_y, the structure remains quite homogeneous for gel solicited close to t_g (strong strain hardening) and very in-homogeneous for gel solicited far away from t_g (low strain hardening).

To do list: further analysis of the experimental data

- Fig. 6 check for anisotropy. Is anisotropy the reason why the data is dirty at low a q? I doubt it since the noise is still present at low γ_0.
- Analyse similar data to Fig. 6 at other t/t_g. Especially compare the results when there is no strain hardening observed at large t/t_g
- plot properly and discuss video rheo in Fig. 7.

V. DISCUSSION

Both the linear mechanical and structure structural properties of the three different dispersion can be mapped on a single master curve. Those quantities therefore do not directly help us foresee the difference in the non-linear mechanics, i.e. a strain hardening effect that is all the more pronounced that it is measured just after t_g and the particles building the gel are small.

To apprehend those results we are currently collaborating with Emanuela Del Gado who tackles this issue using computer simulations. The advantage of those experiments is that since the evolution of the strain hardening happens during the maturation of the gel, the interactions between the particles and the volume fraction constant and therefore allowing us to pinpoint structural quantities that drive the phenomena. Using simulations, we will address the following questions:

- What is the origin of strain hardening in such gels? Two hypothesis are under exploration. (i) as in

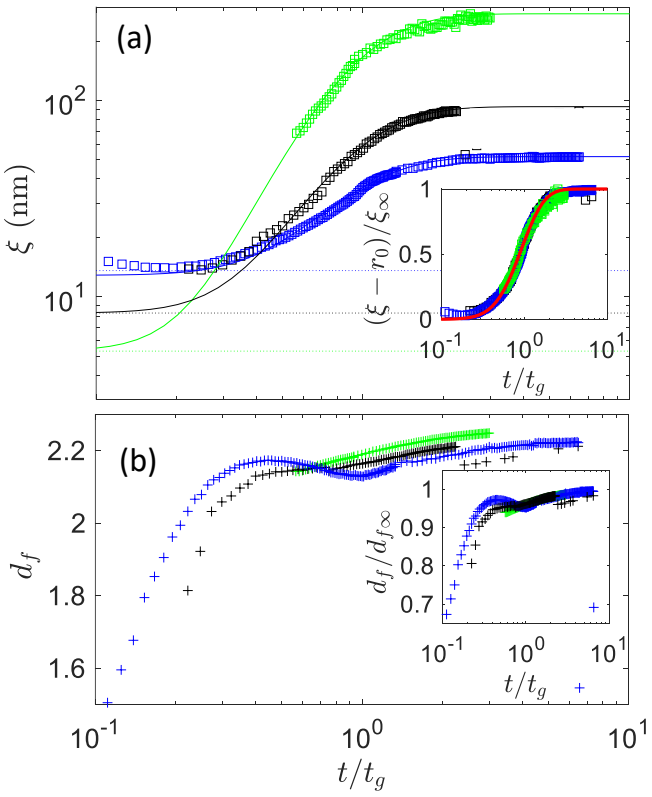

FIG. 5. Structure parameters extracted from the mass fractal fit for the three ludox dispersion SM (green), TM (blue) and HS (black) as a function of the normalized time t/t_g. (a) Evolution of the cluster size ξ. Inset: Evolution of the normalized cluster size. The red line is the master curve $(\xi - r_0)/\xi_\infty = 1 - \exp(-2t/t_g)^{4.5}$ that best fit the data. (b) Evolution of the cluster fractal dimension d_f as function of the normalized time t/t_g. Inset: normalized evolution of d_f/d_∞.

biopolymer gels, the strain hardening could be imputed to the bending modulus of the gel strand. Small colloids form thick strain with a large bending modulus whereas large colloid form thin strand with a small bending modulus. The unbending of the strand leads to a strain hardening all the more important that the bending modulus is strong. (ii) strain hardening could also be linked to the connectivity of the gel network

- Why the strain hardening important just after t_g and decreases thereafter?

- Is there a structural parameter that allows us to rationalize the strain hardening parameter $\Delta G'/G_0$ that could replace the time axis in Fig. 5

[1] M. Gardel, J. H. Shin, F. MacKintosh, L. Mahadevan, P. Matsudaira, and D. A. Weitz, Science **304**, 1301 (2004).
[2] K. Schmoller, P. Fernandez, R. Arevalo, D. Blair, and A. Bausch, Nature communications **1**, 1 (2010).
[3] C. Storm, J. J. Pastore, F. C. MacKintosh, T. C. Lubensky, and P. A. Janmey, Nature **435**, 191 (2005).
[4] T. Gisler, R. C. Ball, and D. A. Weitz, Physical review letters **82**, 1064 (1999).
[5] B. Keshavarz, T. Divoux, S. Manneville, and G. H. McKinley, ACS Macro Letters **6**, 663 (2017).
[6] G. de Oliveira Reis, T. Gibaud, B. Saint-Michel, S. Manneville, M. Leocmach, L. Vaysse, F. Bonfils, C. Sanchez, and P. Menut, Journal of colloid and interface science **539**, 287 (2019).
[7] J. M. van Doorn, J. E. Verweij, J. Sprakel, and J. van der Gucht, Physical review letters **120**, 208005 (2018).
[8] M. Bouzid and E. Del Gado, Langmuir **34**, 773 (2018).
[9] J. Teixeira, Journal of Applied Crystallography **21**, 781 (1988).

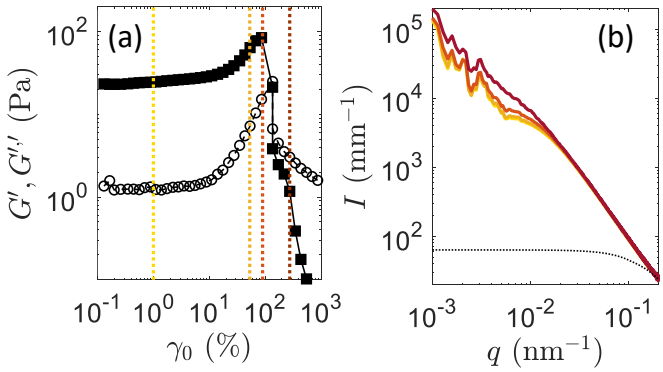

FIG. 6. Strain hardening observation under rheo-TRUSAXS. (a) Strain sweep measurements. (b) $I(q, \gamma_0)$. The color codes for γ_0

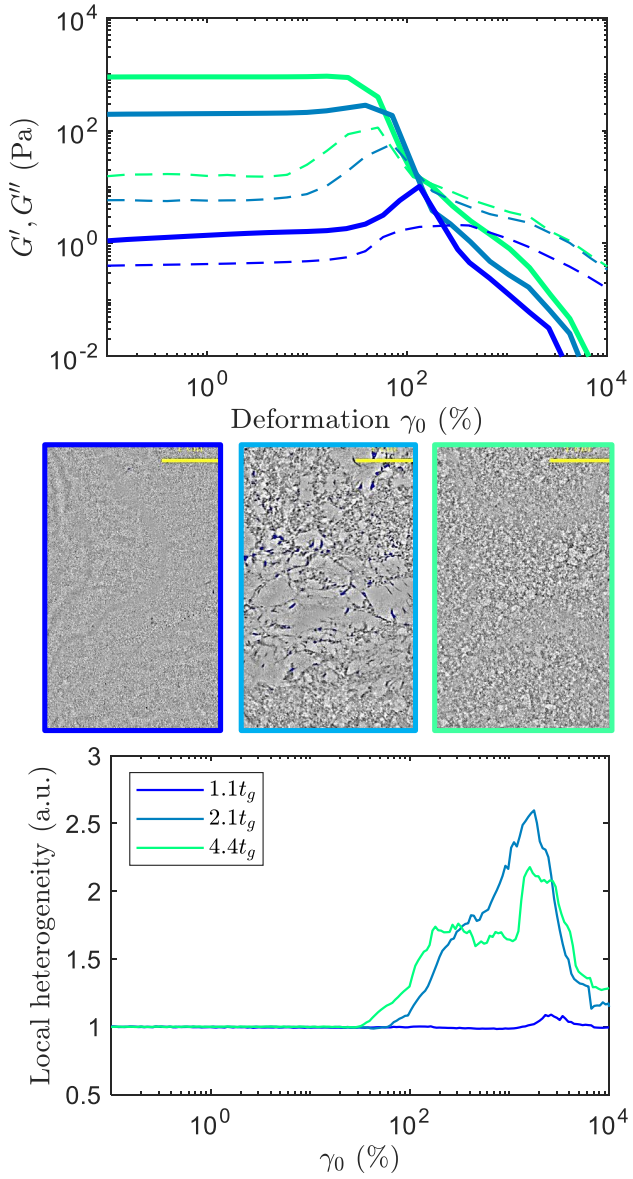

FIG. 7. video rheo.